Slow Self-Activation Enhances The Potency of Viridin Prodrugs

Joseph Blois,[†,#] Hushan Yuan,[†,#] Adam Smith,[†] Michael E. Pacold,[†,‡] Ralph Weissleder,[†,§,||] Lewis C. Cantley,[||,⊥] and Lee Josephson*[,†]

Center for Molecular Imaging Research, Massachusetts General Hospital and Harvard Medical School, 149 13th Street, Charlestown, Massachusetts 02129, Center for Cancer Research, Massachusetts Institute of Technology, 40 Ames Street, Cambridge, Massachusetts 02142, Center for Systems Biology, Massachusetts General Hospital, Boston, Massachusetts 02114, Department of Systems Biology, Harvard Medical School, 200 Longwood Avenue, Boston Massachusetts 02115, Department of Systems Biology, Harvard Medical School and Division of Signal Transduction, Beth Israel Deaconess Medical Center, 77 Avenue Louis Pasteur, Boston Massachusetts 02115

Received April 2, 2008

When the viridin wortmannin (Wm) is modified by reaction with certain nucleophiles at the C20 position, the compounds obtained exhibit an improved antiproliferative activity even though a covalent reaction between C20 and a lysine in the active site of PI3 kinase is essential to Wm's ability to inhibit this enzyme. Here we show that this improved potency results from an intramolecular attack by the C6 hydroxyl group that slowly converts these inactive prodrugs to the active species Wm over the 48 h duration of the antiproliferative assay. Our results provide a guide for selecting Wm-like compounds to maximize kinase inhibition with the variety of protocols used to assess the role of PI3 kinase in biological systems, or for achieving optimal therapeutic effects in vivo. In addition, the slow self-activation of WmC20 derivatives provides a mechanism that can be exploited to obtain kinase inhibitors endowed with physical and pharmacokinetic properties far different from man-made kinase inhibitors because they do not bind to kinase active sites.

Introduction

Viridins, a class of compounds isolated from fungi of which wortmannin (Wm) is a member, have long intrigued pharmacologists because of their potent antiproliferative and immune suppressive properties.[1] Viridins are steroid-like molecules, which have a "extra" furan ring as a common, key structural feature.[1] Wm, the most commonly used viridin, has been widely employed to define the role of PI3 kinase and the PI3 kinase pathway in many biological systems. Wm is a nanomolar PI3 kinase inhibitor,[2,3] but at higher concentrations inhibits polo-like kinase,[4] mTOR,[5] DNA-dependent protein kinase,[6] and ATM.[7] Unlike man-made PI3 kinase inhibitors,[8–11] a specific carbon on Wm, C20, reacts with a lysine in the ATP site of PI3 kinase.[1,12,13] Wm's antiproliferative and immune suppressive activities have been explored over the years beginning in 1974,[14–20] and it continues to be used as a scaffold for drug development.[21,22] Although viridins have been widely used to define the role of the PI3 kinase pathway and for drug development, relationships between viridin chemistry (structure, stability, chemical reactivity) on the one hand, and their bioactivity on the other hand, are sometimes not easily reconciled.

A seeming inconsistency involves the bioactivity of Wm derivatives made by reaction of the electrophilic C20 carbon with nucleophiles: because a covalent reaction between the C20 of Wm and PI3 kinase is an essential part of its mechanism of kinase inhibition, can a reaction between C20 and nucleophiles yield WmC20 derivatives that are more potent than Wm? Early work found that a variety of Wm derivatives made by modification of the electrophilic C20 (see Figure 1 for numbering) with a variety of constituent groups were inactive as PI3 kinase inhibitors and in cell-based assays.[14,23–25] These studies indicated an essential role for an intact C20 in the bioactivity of Wm and suggested C20 might covalently react with an amino acid in the active site of a target enzyme. Indeed, a covalent modification of the catalytic subunit of PI3 kinase by Wm was then reported, followed by crystallographic studies showing a modified Wm in the ATP site.[12,13] Despite these findings on the crucial role played by the intact C20, more recent studies have found Wm derivatives modified at C20 were markedly superior to the starting Wm, both as PI3 kinase inhibitors and in their antiproliferative activity.[22,26]

We hypothesized that the bioactivities of WmC20 compounds might be related to the ability of WmC20 derivatives to form Wm;[27] that is the bioactivity of a WmC20 derivative might reflect a combination of the rate of Wm self-activation and the duration of the assay involved. In this view, cell-based bioassays using long incubation times, (e.g., a 48 h antiproliferative assay), would be more indicative of antiproliferative activity of WmC20 modified compounds in vivo, where sustained, long-term effects are generally defined as efficacy. To investigate this possibility, we modified a recently developed fluorescent Wm[29] with various constituent groups at C20, to obtain a panel of fluorescent WmC20 derivatives that formed the original fluorescent Wm at widely different rates. We then examined the activity of the panel with a short duration PI3 kinase assay and a long duration antiproliferative assay and employed these compounds' fluorescence to determine their fates in cultured cells. We show that certain Wm derivatives modified at C20 (WmC20 derivatives) are poor PI3 kinase inhibitors yet exhibit enhanced potency with a 48 h antiproliferative assay due to a self-activation mechanism that yields the active Wm. As the chemistry of Wm and its derivatives becomes fully understood, these unique natural products can be better exploited to define

* To whom correspondence should be addressed. Phone: (617) 726-6478. Fax: (617) 726-5708. E-mail: josephso@helix.mgh.harvard.edu.
† Center for Molecular Imaging Research, Massachusetts General Hospital and Harvard Medical School.
‡ Center for Cancer Research, Massachusetts Institute of Technology.
§ Center for Systems Biology, Massachusetts General Hospital.
|| Department of Systems Biology, Harvard Medical School.
⊥ Department of Systems Biology, Harvard Medical School and Division of Signal Transduction, Beth Israel Deaconess Medical Center.
# Contributed equally to this work.

10.1021/jm800374f CCC: $40.75
Published on Web 07/17/2008

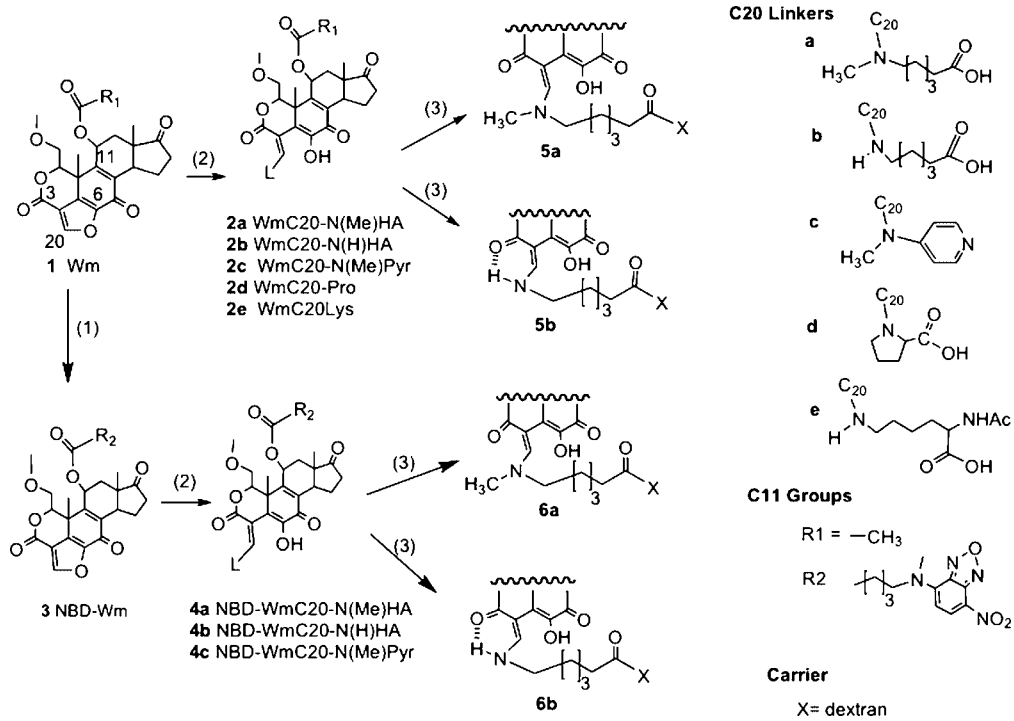

Figure 1. Synthesis of WmC20 compounds. The positions of the C3, C6, C11, and C20 carbons are shown for Wm, **1**. **1** was modified at C11 by the attachment of NBD and a 6-carbon linker to obtain NBD-Wm, **3**. Then **3** was then modified at C20 by the attachments of certain linkers (L's), to yield self-activating fluorescent WmC20 derivatives. An intramolecular attack of the hydroxyl at C6 provides a mechanism of self-activation and Wm generation as in Figure 1 of ref 27. Structures of Linkers attached to C20 (a−e) are provided. The C_{20} designation indicates the point of attachment to NBD-Wm or Wm. The physical properties of low-molecular-weight fluorescent derivatives (**4a**, **4b**) were transformed by reaction with a carrier amino dextran to form **6a** and **6b**. Oxygens at C3 and C6 flanking C20 form hydrogen bonds when Wm (or NBD-Wm) has reacted with a lysine in the ATP binding site of PI3 kinase gamma, see discussion regarding Figure 4. Synthetic Methods: (1) see ref 29; (2) for **2a** and **4a**, 6-methylaminohexanoic acid (N(Me)HA), for **2b** and **4b**, 6-aminohexanoic acid (N(H)HA), for **2c** and **4c**, 4-methylaminopyridine (N(Me)Pyr), for **2d**, L-proline (Pro), for **2e**, *N*-acetyl lysine (Lys)), triethylamine, DMSO, room temperature; (3) (a) for **5a**, **2a**, (for **6a**, **4a**; for **5b**, **2b**; for **6b**, **4b**), *N*-hydroxysuccinimide, 1,3-diisopropylcarbodiimide; (b) aminodextran, DMSO, PBS, pH 7.0, 37 °C.

the role of the PI3 kinase in biological systems or to obtain compounds with acceptable efficacy and toxicity for use in vivo.

Materials and Methods

Compound Synthesis. The strategy employed and compounds synthesized are shown in Figure 1. Compounds **3**, **2a**, **2b**, **2d**, and **2e** were prepared as described.[27−29] Wortmannin (Wm) was a gift of the natural products branch of the National Cancer Institute. Amino-dextran was a 70 kDa species from Invitrogen, Carlsbad, CA. All reagents and solvents were of standard quality. NMR was performed on a Varian 400 MHz and Varian Unity Inova 500 MHz instruments with $CDCl_3$. High resolution mass spectra were obtained on a Micromass LCT instrument by using the time-of-flight ESI technique. Low resolution mass spectra were collected on a Waters Micromass ZQ MAA288 instrument. Compounds were purified by HPLC (Varian Prostar 210 with a variable wavelength PDA 330 detector), which employed reverse phase C18 columns (VYDAC, catalogue no. 218TP1022 for preparative work; Varian, catalogue no. R0086200C5 for analytical work) with water (Millipore, containing 0.1% trifluoroacetic acid) (buffer A), and acetonitrile (containing 20% buffer A) (buffer B) as the elution buffers. System 1 (for **2c** and **4c**): buffer A:buffer B (70:30) linear gradient to buffer A:buffer B (0:100) over 15 min, then gradient back to 70:30 (buffer A:buffer B) for 3 min and isocratic for 5 min; flow: 1.0 mL/min; λ_{max}: 410 and 495 nm. System 2 (for **2c** and **4c**): buffer A:buffer B (70:30) linear gradient to buffer A:buffer B (0:100) over 20 min, isocratic for 5 min, then gradient back to 70:30 (buffer A:buffer B) for 5 min and isocratic for 5 min; flow: 4.9 mL/min; λ_{max}: 410 and 495 nm. System 3 (for **4a**): buffer A:buffer B (80:20) isocratic for 5 min, linear gradient to buffer A:buffer B (20:80) over 30 min, then gradient back to 80:20 (buffer A:buffer B) for 5 min and isocratic for 5 min; flow: 6.0 mL/min; λ_{max}: 410 nm. System 4 (for **4b**): buffer A:buffer B (80:20) isocratic for 5 min, linear gradient to buffer A:buffer B (20:80) over 30 min, then isocratic for 5 min, gradient back to 80:20 (buffer A:buffer B) for 5 min and isocratic for 5 min; flow: 6.0 mL/min; λ_{max}: 408 nm. System 5 (for **4a**): buffer A:buffer B (70:30) linear gradient to buffer A:buffer B (0:100) over 25 min, then isocratic for 5 min and gradient back to 70:30 (buffer A:buffer B) in 5 min and isocratic for 5 min; flow: 1.0 mL/min; λ_{max}: 280 and 490 nm. System 6 (for **4b**): buffer A:buffer B (50:50) linear gradient to buffer A:buffer B (23:77) over 20 min, then isocratic for 5 min and gradient back to 50:50 (buffer A:buffer B) in 5 min and isocratic for 5 min; flow: 1.0 mL/min; λ_{max}: 280 and 490 nm.

Synthesis of 2c. A mixture of Wm **1** (12 mg, 0.028 mmol) and 4-(*N*-methylamino) pyridine (60 mg, 0.55 mmol) in anhydrous CH_2Cl_2 (1 mL) was stirred at room temperature for 15 h. The mixture was purified by preparative silica gel TLC developed by CH_2Cl_2:MeOH (10:1). A dark-yellow solid was obtained. Crude yield: 40% with purity 96% (system 1). A further HPLC purification (system 2) was needed for both the PI3 kinase enzyme and antiproliferative cell-based assays. A bright-yellow powder (**2c**) would be obtained after lyophilization. HRMS: $C_{29}H_{32}N_2O_8$, expt 537.2237 ($M + H^+$), obsd. 537.2220. LRMS: 537.0. ^{1}H NMR ($CDCl_3$, ppm, 500 MHz): δ 0.86 (3H, s, C13-CH_3), 1.24 (1H, br, OH), 1.64 (3H, s, C10-CH_3), 1.79−1.84 (1H, q, $J_1 = 5.2$ Hz, $J_2 = 14.3$ Hz, H-12), 2.04−2.12 (4H, m, H-15, $OCCH_3$), 2.24−2.29 (1H, m, H-16), 2.39−2.44 (1H, q, $J_1 = 7.4$ Hz, $J_2 = 14.3$ Hz, H-12), 2.53−2.62 (1H, m, H-16), 2.89−3.02 (2H, m, H-14, OCH_2), 3.11−3.17 (4H, m, H-15, N-CH_3), 3.25 (3H, s, OCH_3), 3.27−3.32 (1H, q, $J_1 = 2.19$ Hz, $J_2 = 11.0$ Hz, OCH_2), 4.61−4.63 (1H, q, $J_1 = 2.5$ Hz, $J_2 = 6.6$ Hz, H-1), 6.07−6.10 (1H, m, H-11), 7.00 (2H, d, $J = 6.4$ Hz, Py-H), 8.39 (1H, s, H-20), 8.35 (2H, d, $J = 6.4$ Hz, Py-H).

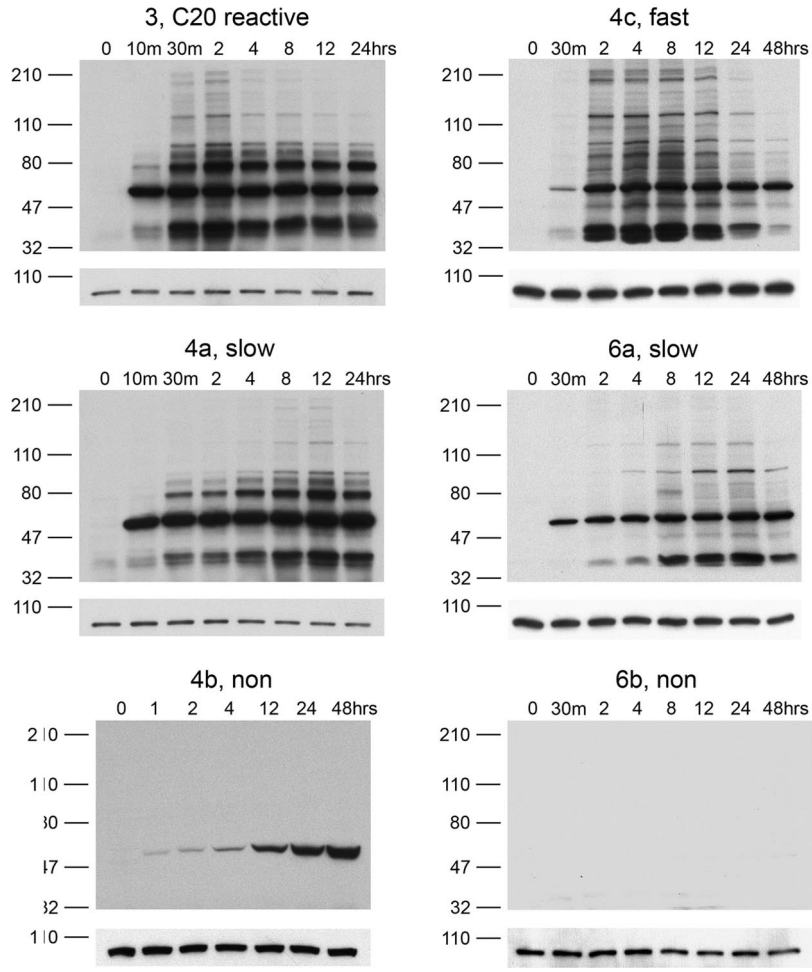

Figure 2. Time course for NBD-Wm cell protein labeling when cells were incubated with C20 reactive NBD-Wm or NBD-WmC20 compounds with various rates of self-activation. Cells were incubated with 10 μM of NBD-Wm, either as NBD-Wm or a WmC20 derivative with various rates of self-activation for specified times and lysed. After SDS electrophoresis, NBD-modified proteins were visualized with an anti-NBD Western blot method as described.[29] Wortmannylated (NBDylated) proteins were seen with the principal bands at 35 kDa (possibly a doublet), 55 kDa, and 75 kDa. With all compounds the 55 kDa band appeared first. Time course of cell protein labeling (total area of 35, 55, and 75 kDa bands from densitometry) was further analyzed and is shown in Figure 3A.

Synthesis of 4a. NBD-Wm **3** (43.8 mg, 0.065 mmol), 6-(*N*-methylamino)-hexanoic acid hydrogen chloride (53 mg, 0.3 mmol), and triethylamine (40 μL) were mixed in anhydrous DMSO (2 mL). The mixture was stirred at room temperature and completed immediately. After dilution with 50% acetonitrile in water (1:1) before the injection, the mixture was purified by HPLC (system 3) and gave a red powder after lyophilization. Analysis of **4a** by HPLC (system 5) showed less than 3% of NBDWm: 38.1 mg, 67.6%. HRMS: $C_{41}H_{51}N_5O_{13}$, calcd 822.3561 ($M + H^+$), found 822.3594. LRMS: 822.4. ^{1}H NMR ($CDCl_3$, ppm, 400 MHz): δ 0.86 (3H, s, C13-CH_3), 1.42−1.48 (4H, m, $NCH_2CH_2CH_2CH_2CH_2CO$), 1.56 (3H, s, C10-CH_3), 1.61−1.78 (9H, m, $NCH_2CH_2CH_2CH_2CH_2CO$, H-12), 2.05−2.16 (1H, m, H-16), 2.22−2.47 (4H, m $NCH_2CH_2CH_2CH_2CH_2CO$), 2.54−2.64 (1H, m, H-15), 2.73−2.87 (3H, m, H-12, H-14, H-16), 2.92−2.99 (1H, m, OCH_2), 3.09−3.17 (1H, m, H-15), 3.22 (3H, s, OCH_3), 3.30−3.60 (11H, br, NCH_3, OCH_2, NCH_2, OH), 4.08 (2H, br, $ArNCH_2$), 4.48−4.49 (1H, d, J = 6.25 Hz, H-1), 6.07−6.13 (2H, m, H-11, ArH), 8.26 (1H, s, H-20), 8.46 (1H, d, J = 9.0 Hz, ArH).

Synthesis of 4b. NBD-Wm **3** (13 mg, 0.02 mmol) and 6-amino-hexanoic acid (13 mg, 0.1 mmol) were mixed in anhydrous DMSO (1 mL). The mixture was stirred at room temperature for 1.5 h. After dilution with 50% acetonitrile in water (1:1) before the injection, the mixture was purified by HPLC (system 4) and gave a red powder after lyophilization. HPLC analysis (System 6) showed a single peak to prove its high purity; 13.5 mg, 83.9%. HRMS: $C_{40}H_{49}N_5O_{13}$, calcd 808.3405 ($M + H^+$), found 808.3423. LRMS: 808.4 ($M + H^+$), 825.4 ($M + NH_4^+$), 830.4 ($M + Na^+$). ^{1}H NMR ($CDCl_3$, ppm, 400 MHz): δ 0.82 (3H, s, C13-CH_3), 1.42−1.50 (4H, m, $NCH_2CH_2CH_2CH_2CH_2CO$), 1.52 (3H, s, C10-CH_3), 1.67−1.82 (9H, m, $NCH_2CH_2CH_2CH_2CH_2CO$, H-12), 2.22−2.42 (7H, m, $NCH_2CH_2CH_2CH_2CH_2CO$, H-12, H-15, H-16), 2.53−2.61 (1H, m, H-16), 2.73−2.95 (2H, H-14, OCH_2), 3.14−3.18 (1H, m, H-15), 3.23 (3H, s, OCH_3), 3.39−3.68 (8H, m, br, NCH_3, NCH_2, OCH_2, OH), 4.08 (2H, br, $ArNCH_2$), 4.29 (1H, d, J = 7.6 Hz, H-1), 5.99−6.02 (1H, m, H-11), 6.11 (1H, d, J = 9.0 Hz, ArH), 8.46 (1H, d, J = 9.0 Hz, ArH), 8.53 (1H, d, J = 13.9 Hz, H-20), 9.82−9.88 (1H, m, NH). ^{13}C NMR (ppm): 16.65, 22.62, 24.28, 26.02, 26.26, 26.53, 30.42, 33.51, 33.80, 36.62, 38.63, 42.43, 42.50, 43.88, 49.97, 49.98, 55.93, 59.43, 67.51, 73.31, 77.43, 81.31, 88.41, 101.31, 129.05, 135.70, 137.09, 137.56, 145.10, 145.57, 150.83, 159.61, 166.15, 172.62, 177.22, 178.65, 218.10.

Synthesis of 4c. A mixture of NBD-Wm **3** (21 mg, 0.031 mmol) and 4-(N-methylamino) pyridine (0.268 g, 0.6 mmol) in anhydrous CH_2Cl_2 (2 mL) was stirred at room temperature for 2 days. The mixture was purified by preparative silica gel TLC developed by CH_2Cl_2:MeOH (10:1). A dark-red waxy solid was obtained. Crude yield: 16.7% with purity 95% (system 1). A further HPLC purification (system 2) was needed for both the PI3 kinase enzyme and antiproliferative cell-based assays. A bright-red powder (**4c**) would be obtained after lyophilization. HRMS: $C_{40}H_{44}N_6O_{11}$, expt 785.3141 ($M + H^+$), obsd. 785.3145. LRMS: 807.4 [$M + Na^+$]. ^{1}H NMR ($CDCl_3$, ppm, 400 MHz): δ 0.90 (3H, s, C13-CH_3), 1.44−1.49 (2H, m, J = 7.3 Hz, $NCH_2CH_2CH_2CH_2CH_2CO$), 1.62

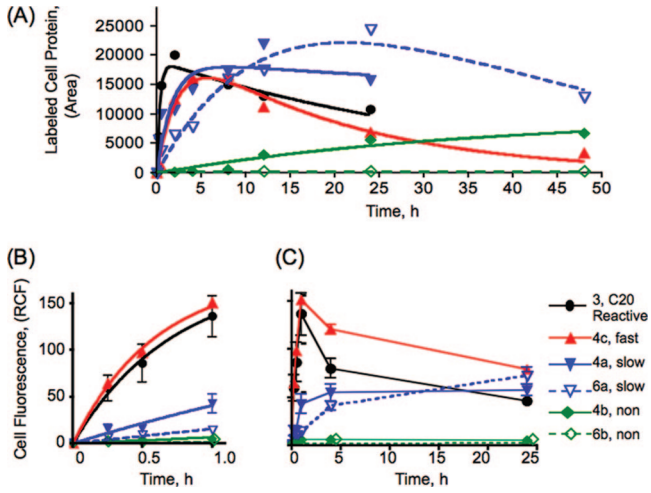

Figure 3. Time courses for the behavior of fluorescent WmC20 derivatives in cells. (A) Time course for the formation of wortmannylated cell protein with the C20 reactive NBD-Wm **3** or NBD-WmC20 compounds. (B) and (C): Time course for cell fluorescence, (uptake of NBD). Relative cell fluorescence, the RCF on the *y*-axis, was the same for the short (B) and long time scales (C). Lines in (A) or (B) were obtained by fitting data to the equations given in Methods, with the relative initial rates given in Table 1. Equivalent concentrations of 10 μM Wm were used throughout.

(3H, s, C10-CH_3), 1.71−1.83 (5H, m, $NCH_2CH_2CH_2CH_2CH_2CO$, H-12), 2.02−2.12 (1H, m, H-15), 2.24−2.34 (1H, m, H-16), 2.37 (2H, t, J = 7.32, $NCH_2CH_2CH_2CH_2CH_2CO$), 2.45−2.49 (1H, q, J_1 = 7.32 Hz, J_2 = 13.7 Hz, H-12), 2.57−2.63 (1H, q, J_1 = 8.8 Hz, J_2 = 19.5 Hz, H-16), 2.66 (1H, s, OH), 2.92−2.98 (2H, m, H-14, OCH_2), 3.17−3.19 (1H, m, H-15), 3.20 (3H, s, OCH_3), 3.21 (3H, s, N-CH_3), 3.34−3.37 (1H, q, J_1 = 2.9 Hz, J_2 = 10.7 Hz, OCH_2), 3.46 (3H, br, NCH_3), 4.12 (2H, br, NCH_2), 4.73−4.74 (1H, q, J_1 = 2.9 Hz, J_2 = 5.9 Hz, H-1), 6.10−6.13 (2H, m, H-11, NBD-H), 7.22 (2H, d, J = 6.8 Hz, Py-H), 8.26 (1H, s, H-20), 8.46 (1H, d, J = 8.8 Hz, NBD-H), 8.63 (2H, d, J = 6.8 Hz, Py-H).

Synthesis of 5a. To an amino-dextran (300 mg, 0.00429mmol) in 4 mL PBS, pH 7 was added to the NHS ester of **2a** in 4 mL DMSO (28.7 mg, 0.0429 mmol), and the mixture incubated for 1.5 h at 37 °C. Low-molecular-weight impurities were removed with Sephadex G-50 chromatography in 1 mM phosphate buffer at pH 7.0. A yellow powder was obtained after lyophilization. The Wm attached was determined from Wm absorbance by using UV standard curves at 418 nm. The ratio of **2a** to dextran was 5.9.

Synthesis of 5b. Amino-dextran (202 mg, 0.00429mmol) in 3 mL PBS, pH 7 was added to the NHS ester of **2b** in 5 mL DMSO (56 mg, 0.0858 mmol), and the mixture incubated for 3 h at 37 °C. Low-molecular-weight impurities were removed as above, and a yellow powder was obtained after lyophilization. The Wm attached was determined from Wm absorbance by using UV standard curves at 408 nm. The ratio of **2b** to dextran was 7.6.

Synthesis of 6a. To a 70 kDa amino-dextran (35 mg, 0.0005mmol) in 1 mL PBS, pH 7 was added to the NHS ester of **4a** in 4 mL DMSO (6.6 mg, 0.00718 mmol) and the mixture incubated for 2 h at 37 °C. Low-molecularweight impurities were removed with lyophilization as above. The NBD-Wm **3** attached was determined from NBD absorbance by using UV standard curves at 490 nm. The ratio of **4a** to dextran was 3.7.

Synthesis of 6b. Amino-dextran (36 mg, 0.0005 mmol, 70 kDa) was reacted with the NHS ester of **4b** (5.5 mg, 0.005 mmol) and purified as above. The ratio of **4b** to dextran was 6.3.

Dextran interfered with the PI3 kinase assay (data not shown), so the ability of **5a**, **5b**, **6a**, and **6b** to inhibit PI3 kinase was obtained with compounds where an amino glucose carrier replaced the amino dextran. The NHS ester of **2a** (or **2b**, **4a**, **4b**) (0.04 mmol) was mixed with 2-amino glucose hydrogen chloride (0.4 mmol) in anhydrous DMSO (1 mL). After the addition of triethylamine (60 μL), the mixtures were incubated under 37 °C for 2.5 h. The solution was diluted with water (1 mL) and applied to HPLC using system 5: buffer A:buffer B (90:10) linear gradient to buffer A:buffer B (40:60) over 25 min, then isocratic for 5 min and gradient back to 90:10 (buffer A:buffer B) in 5 min and isocratic for 5 min; flow: 4.9 mL/min; λ_{max}: 280 and 410 nm. Yield: 65−80%. HRMS: **7a**: $C_{36}H_{50}N_2O_{14}$ expt 735.3335 [M + H^+], obs 735.3325; LRMS 757.4 [M + Na^+]. **7b**: $C_{35}H_{48}N_2O_{14}$ expt 721.3178 [M + H^+], obs 721.3176; LRMS 743.4 [M + Na^+]. **8a**: $C_{47}H_{62}N_6O_{17}$ expt 983.4244 [M + H^+], obs 983.4256; LRMS 1005.4 [M + Na^+]. **8b**: $C_{46}H_{60}N_6O_{17}$ expt 991.3907 [M + Na^+], obs 991.3914; LRMS 991.7 [M + Na^+].

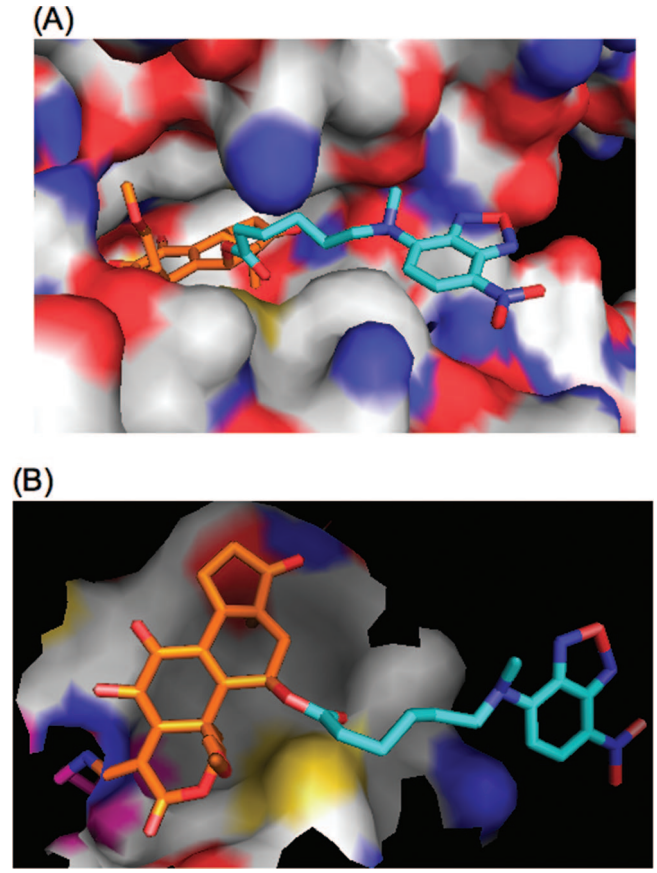

Figure 4. Binding of NBD-Wm 3 into the active site of PI3 kinase gamma. Model is based on the published structure of Wm in the ATP site of PI3 kinase gamma (PDB: 1E7U) with NBD adduct added. (A) Desacyl Wm (Wm lacking the acetyl group at C11) is orange. The NBD adduct (NBD and six carbon linker) is colored cyan, with nitrogen in blue and oxygen in red. The NBD and the six-carbon linker protrude out of the ATP-binding pocket into the solvent while Wm is buried deeply in the ATP-binding pocket. (B) Another view of NBD-Wm showing the relationship between the surface of the enzyme and NBD-Wm. Lysine 833, covalently reacted with the C20 of Wm, is in magenta and extends through a blue, positively charged surface. The proximity of the surface prevents Wm derivatives modified at C20 from binding in the ATP-binding pocket.

Generation of Wm or NBD-Wm 3. The half-times for Wm formation were determined by incubating WmC20 compounds at 1.5 mM Wm equivalents in PBS, pH 6.8, and 37 °C. The mixture was analyzed by HPLC using MHB as an internal standard (1 μg of methyl-4-hyrdroxybenzoate). With **4a**, **4b**, and **4c**, 10% acetonitrile and 5% DMSO were added to ensure solubility of the NBD-Wm that was formed. System 1 (for **2c** and **4c**), system 5 (for **4a**), and system 6 (for **4b**) were used for HPLC analysis. With the WmC20 dextran conjugates of Wm and NBD-Wm insolubility was utilized as a separation mechanism. A solution of **5a** or **6a** (1.5 mM Wm equivalents) in 300 μL in PBS (pH 7.0) was incubated at 37 °C. For **5a**, release was monitored by a decrease in absorbance at 322 nm that occurs with Wm formation. For **6a**, released NBD-

Table 1. Wm Formation and Activities of WmC20 Compounds[a]

compound	R group[b]@ C11	linker (L) [b]@ C20	carrier[b]	half-time of Wm or NBD-Wm formation (h)	PI3K IC50 (μM)	antiprolif. [c]IC50 (μM)	cell protein labeling, relative initial rate	cell uptake, relative initial rate
1	acetyl,R1	none	no	not applicable	0.0176 ± 0.017	11.4 ± 0.5		
3	NBD,R2	none	no	not applicable	0.0242 ± 0.016	12.2 ± 0.8	1.00	1.00
2c	*R1*	*N(Me)-Pyr, (c)*	*no*	*2.30 (2.13−2.42)*	*0.119 ± 0.011*	*9.86 ± 2.52*		
4c	*R2*	*(c)*	*no*	*1.87 (1.69−2.73)*	*0.262 ± 0.020*	*9.99 ± 1.25*	*0.206*	*1.199*
2a	**R1**	**N(Me)-HA,(a)**	**no**	**8.7 (7.83−9.75)**	**0.128 ± 0.016**	**0.96 ± 0.33**		
4a	**R2**	**(a)**	**no**	**8.0 (6.96−9.53)**	**0.174 ± 0.012**	**3.85 ± 0.36**	**0.246**	**0.187**
2d	**R1**	**Pro, (d)**	**no**	**9.9 (7.29−15.53)**	**0.105 ± 0.011**	**1.79 ± 0.18**		
5a	**R1**	**(a)**	**yes**	**9.1 (7.42−11.65)**	**0.458 ± 0.021**	**1.05 ± 0.42**		
6a	**R2**	**(a)**	**yes**	**9.2 (8.54−10.08)**	**0.453 ± 0.017**	**1.04 ± 0.10**	**0.0656**	**0.0661**
2b	R1	(b)	no	>100	>10	27.9 ± 3.3		
4b	R2	(b)	no	>100	>10	48.7 ± 13.3	0.00613	0.0271
5b	R1	(b)	yes	>100	>10	not detected		
6b	R2	(b)	yes	>100	>10	not detected	none	0.0064
2e	R2	NAclys, (e)	no	>100	>10	29.8 ± 0.9		

[a] Non-C20 protected compounds(**1** and **3**) are given first, followed by WmC20 derivatives grouped from top to bottom by half-times of Wm formation. [b] Structures of compounds, R groups at C11 and linkers L at C20, as well abbreviations used for linkers, are provided in Figure 1 and its legend. [c] Antiprolif. is the antiproliferative assay.

Wm was removed by centrifugation (5 min, 13000 rpm, Eppendorf benchtop microfuge). The absorbance of the supernatant at 480 nm was used to obtain NBD-Wm released. Absorbances (322 or 480 nm) were fit to a first-order decay process (log absorbance versus time), with coefficients of correlation of greater than 0.95 in all cases. First-order decay constants were converted to half-times.

Activity-Based Bioassays. The antiproliferative assay employed sulforhodamine B binding to determine cell mass as described.[29] The PI3 kinase assay employed the gamma catalytic subunit of PI3 kinase and was the fluorescence energy transfer assay.[30] The human, nonsmall cell lung carcinoma A549 cell line was used in the cell proliferation assay, cell pharmacokinetic assays, and as a tumor model, that is, for all studies reported here. All concentrations are expressed as moles of Wm.

Cellular Pharmacokinetics. NBD-Wm cell protein labeling assay: Cells were treated with 10 μM of NBD-Wm **3** or an NBD-WmC20 derivative for the indicated time and whole cell lysates generated. Cell protein was normalized between samples and wortmannylated (NBDylated) protein was visualized using an anti-NBD rabbit polyclonal antibody (Biogenesis, Munich, Germany) as described[29] and quantified using densitometry. Labeled cell protein was taken as the sum of the areas of three prominent bands (35, 55, and 75 kDa). Values of labeled cell protein as a function of time ($L(t)$) were fit to a two step sequential model where k_1 was the rate of increase of labeled protein, k_2 was the rate of decrease of labeled protein, and L_0 was the maximum using GraphPad Prism Software (Irvine, CA): $L(t) = L_0 \times k_1/(k_2 - k_1)\ \exp((-k_1 t) - \exp(-k_2 t))$. Initial rates were the increase in $L(t)$ over the initial 5 min of reaction as shown in Figure 3A normalized to fastest compound.

Cellular Pharmacokinetics, NBD-Wm Cell Uptake Assay by Fluorescence. Cells were incubated with 10 μM of **3** or an NBD-WmC20 derivative for the indicated time. Cells were detached with trypsin and fluorescence determined by FACS.[29] Cell fluorescence as a function of time ($F(t)$) was measured as the relative cellular fluorescence (RCF), which is the geometric mean of cells exposed to an NBD compound divided by geometric mean of unexposed cells.[29,31,32] All data for the first hour were fit to a single exponential curve ($F(t) = F_0(1 - \exp - kt$). Initial rates were the increase in $F(t)$ over the initial 5 min of reaction as shown in Figure 3B normalized to fastest compound.

The X-ray crystal structure of Wortmannin bound to PI3K gamma (1E7U12) was loaded into PyMOL (DeLano, W.L. The PyMOL Molecular Graphics System (2002), DeLano Scientific, Palo Alto, CA) and the 6-carbon linker and NBD were attached using the PyMOL Build function.

Results

Our strategy for the synthesis of Wm-based viridin derivatives is shown in Figure 1. Low-molecular-weight WmC20 derivatives were prepared by reacting the C20 of NBD-Wm **3** or Wm **1**, which behave similarly as PI3 kinase inhibitors and in the antiproliferative assay,[29] with nucleophiles. This yielded low-molecular-weight WmC20 derivates **2a**−**e** (from **1**) and **4a**−**c** (from **3**). The modification of Wm at C11 for NBD attachment and the modification at C20 occur independently. Low-molecular-weight WmC20 derivatives featuring a carboxylic acid (**2a**, **4a**, **2b**, and **4b**) were then reacted with the amino group of a 70 kDa amino-dextran, which increases their molecular weight and increases their hydrophilicity through an association with many hydroxyls on the polyglucose-like dextran polymer.

The half-times of Wm formation of the 12 WmC20 compounds shown in Figure 1 were then determined. Compounds featuring a N(Me)pyridine group at C20 (**2c** and **4c**) had half-times for Wm formation of 2.30 and 1.87 h, respectively. These compounds are termed "fast Wm forming" WmC20 derivatives and are shown in italics in Table 1. Five WmC20 derivatives featured an alkyl-based tertiary enamine at C20 (**2a**, **2d**, **4a**, **5a**, and **6a**) and formed Wm with half-times between 8.0 and 9.9 h. These compounds are termed "slow Wm forming" WmC20 compounds and are shown in bold lettering in Table 1. Five WmC20 compounds featuring a secondary enamine at C20 (**2b**, **2e**, **4b**, **5b**, and **6b**) were termed "non-Wm-forming" WmC20 derivatives. With these compounds the formation of Wm could not be detected (less than 2% of the WmC20 compound) after 10 h in PBS, our standard assay, or when the incubation period was extended to 100 h. On the basis of their behavior under these conditions, they are termed "non-Wm formers," although Wm formation might occur below our detection limits or in biological systems. They are listed as having half-times of greater than 100 h in Table 1. The designation of WmC20 derivatives as "fast," "slow", or "non" Wm reflected their rate of formation, which in turn was determined by the nature and type of atoms near C20 (leaving group) and which was independent of the group present at C11 (NBD adduct vs acetyl group) or the attachment of dextran attached to the carboxyl group of **2a** and **2b**, or **4a** and **4b**.

We next measured the behavior of fast, slow and non-Wm forming WmC20 compounds using Wm derivatives that lacked modifications at C20, that is Wm **1** and NBD-Wm **3** as controls, in our four bioassays. Data obtained is provided in Table 1.

Activity-Based Antiproliferative and PI3 Kinase Assays. With the antiproliferative assay, fast Wm releasing compounds had IC50s similar to Wm, slow Wm releasing compounds had IC50s 3−12 times lower than the Wm IC50 (better than Wm), and

non-Wm releasers had IC50s at least 2.6 times higher than that of Wm (worse than Wm). With the in vitro PI3 kinase assay on the other hand, all WmC20 compounds tested were notably less effective inhibitors than Wm. Fast or slow Wm releasing compounds had IC50s 5−30 times higher than Wm. Non-Wm formers did not inhibit PI3 kinase even at the highest concentration employed (10 μM). All WmC20 derivatives tested were weaker PI3 kinase inhibitors than Wm, reflecting the incomplete generation of Wm during this 0.5 h assay, with the rate of Wm formation governed by the nature of the leaving group at C20. To ascertain whether the variable rates of Wm formation achieved with our panel of WmC20 derivatives in PBS determined the pharmacokinetics with which compounds interacted with cells, we exposed intact cells to fluorescent WmC20 compounds and determined their fate.

NBD-Wm Cell Protein Labeling. The time course for the formation of wortmannylated cell protein provided a measure of a cell's exposure to the reactive species (NBD-Wm **3**), when an NBD-WmC20 compound was applied to cells. Cells were exposed to 10 μM of the non-C20 protected NBD-Wm or **3**, the fast Wm releasing **4c**, the slow releasing **4a** and **6a**, and the nonreleasing **4b** and **6b** for various times. After lysis, cell protein was subjected to SDS gel electrophoresis and the presence of wortmannylated proteins (NBDylated proteins) determined by reacting the gel with anti-NBD as shown in Figure 2. With all compounds, the 55 kDa band was detected before other bands and was the only band seen with the non-Wm-releasing **4b**. The ability of **4b** to label the 55 kDa protein indicates some NBD-Wm formation was occurring under these conditions (48 h incubation with cells), although **4b** was designated as a "non" Wm forming compound based on its behavior in PBS. This small difference may reflect slightly different activation mechanisms in cells versus PBS or reflect a higher sensitivity of the enzyme amplified Western blot method for detecting wortmannylated protein in Figure 2.

To more quantitatively determine the time course of cell protein labeling, films of Western blots were scanned and areas of the 35, 55, and 75 kDa bands were summed and plotted versus time as shown in Figure 3A, with the relative initial rates of cell protein labeling given in Table 1. The formation of wortmannylated cell protein reflects a reaction between the C20 of Wm, either added as NBD-Wm **3** or released from a NBD-WmC20 derivative (**4a**−**c**, **6a**, **6b**), and the epsilon amino groups of protein lysines. Reactions between Wm and lysine (an N acetylated lysine), including exchange reactions between WmC20 protected derivatives and lysine, occur under physiological conditions in vitro.[28] The decrease of wortmannylated protein with long incubation times likely reflects protein degradation and synthesis. All WmC20 protected compounds labeled protein more slowly than the non-C20 protected NBD-Wm. The low-molecular-weight **4c** labeled protein similarly to **4a**, which in turn was faster than **4b** (**4c** ∼ **4a** > **4b**). The difference between **4a** and **4b** (**4a** > **4b**) was maintained when they were attached to dextran (**6a** > **6b**), although attachment to dextran resulted in a deceased rate of protein labeling (**4a** > **6a** and **4b** >).

NBD-Wm Cell Uptake by Cell Fluorescence. To obtain another measure of the cellular pharmacokinetics of NBD-WmC20 compounds, cells were incubated with these compounds, and the resulting NBD-derived cellular fluorescence as a function of time determined as shown in Figure 3B. Relative initial rates of fluorescence increase, which reflect compound uptake, are provided in Table 1. Here **4c** was taken up faster than **4a**, which was taken up faster than **4b** (**4c** > **4a** > **4b**). Again, this pattern (**4a** > **4b**) maintained when **4a** or **4b** were attached to dextran (**6a** > **6b**), although as with the labeled cell protein assay, dextran attachment resulted in a decreased rate of compound uptake (**4a** > **6a** and **4b** > **6b**).

Discussion

WmC20 Compounds Have Variable Rates of Wm Formation. WmC20 compounds formed Wm at highly variable rates that depended on the nature of the leaving group at C20. With tertiary aromatic enamines such as *N*-methyaminopyridine at C20, the delocalization of electrons by the pyridine ring, together with a tertiary enamine at C20, resulted in half-times for Wm formation of 1.87 and 2.30 h for **2c** and **4c,** respectively (Table 1). With tertiary aliphatic enamines at C20, a slow Wm formation was obtained: half-times were between 8.0 and 9.9 h. Slow Wm forming compounds included N(Me) hexanoic acid (abbreviated N(Me)HA) based WmC20 derivatives (**2a**, **4a**, **5a**, **6a**) and **2d**, which featured a proline leaving group. With secondary enamines at C20, Wm formation was not observed: the half-time for Wm formation was greater than 100 h. Compounds in this class included N(H) hexanoic acid based compounds (**2b**, **4b**, **5b**, **6b**) or **2e**, which featured a lysine leaving group. The rates of Wm release were independent of the presence of the group at C11 (acetyl or NBD-adduct) and the attachment of the low molecular carboxylic acid WmC20 derivatives (**2a**, **2b**, **4a**, **4b**) to a dextran carrier (**5a**, **5b**, **6a**, **6b**). The attachment of low-molecular-weight WmC20 derivatives to dextran increased the size and water solubility of the Wm (data not shown) without altering Wm release kinetics. For example, the half-time for Wm formation with **2a** was 8.7 h, while that for **2a** with dextran attached (**5a**) was 9.1 h.

WmC20 Compounds as Inhibitors of PI3 Kinase. All WmC20 compounds were substantially weaker PI3 kinase inhibitors than Wm, though they fell into two classes. Compounds which did not form Wm (or NBD-Wm), that is **2b**, **4b**, **5b**, **6b**, or **2e**, featured a secondary amine at C20 and failed to inhibit PI3 kinase at the highest concentration employed (10000 nM). Fast Wm forming (**2c**, **4c**) or slow Wm forming compounds (**2a**, **4a**, **5a**, **6a**, **2d**) inhibited the enzyme but with higher IC50s than Wm due to the incomplete production of Wm in the 0.5 h time of the assay. These results were consistent with our earlier work on the inhibition of PI3 kinase by **2a** and **2b**, which used a radioactive lipid phosphorylation assay,[27] while the current study employed a fluorescence energy transfer method.[30]

WmC20 Compounds as Inhibitors of Cell Proliferation. The conclusion that the kinetics of Wm formation controlled the antiproliferative activity of WmC20 compounds was supported by the correlation between the rates of Wm formation and the antiproliferative activities of the WmC20 compounds in culture (Table 1). Fast Wm releasers with half-times for Wm formation of 1.87−2.30 h had IC50s similar to Wm, which were short compared to the 48 h time for the antiproliferative assay and reflects the negligible effect of the Wm formation reaction under these conditions. Slow Wm releasers (half-time for Wm formation about 9 h) had lower IC50s than Wm (more potent than Wm), a behavior we related to their slow generation of Wm over the 48 h time of the assay. On the other hand, non-Wm formers had IC50s higher than Wm. Because their half-times for Wm formation were greater than 100 h, about twice the 48 h assay period, these compounds would be expected to largely remain as inactive C20 modified Wm derivatives for the duration of the assay. Although the rate of Wm formation with WmC20 compounds appeared to explain the activity of these compounds in PI3 kinase and antiproliferative assays, we

sought to confirm that Wm release controlled the pharmacokinetic behavior of these compounds in more complex situations involving cells.

With two assays reflecting the pharmacokinetic interaction of our compounds with cells (formation of NBD-Wm labeled cell protein by anti-NBD-Western blot and uptake of NBD-Wm by cell fluorescence), the widely varying rates of NBD-Wm formation in vitro correlated with the time course obtained (Table 1). Thus the fast Wm forming **4c** entered cells faster than the slowly Wm forming **4a**, which in turn was faster in these respects than the non-Wm forming **4b** (**4c** > **4a** > **4b**). The non-Wm forming compounds **4b** and **6b** exhibited extremely slow pharmacokinetics in cell protein labeling and were poorly internalized by cells. Results with the labeled cell protein assay generally paralleled those with the cell fluorescence assay, the exception being that the rate of cell protein labeling for **4c** was slightly slower than **4a**, although on the basis of Wm formation rates, **4c** should be faster.

The view that the energy for the high affinity between PI3 kinase and Wm is largely derived from the reaction between the electrophilic C20 and a lysine in the ATP site of the catalytic subunit of PI3 kinase stems from observations that Wm when modified at C20 inhibits PI3 kinase either very poorly or not at all,[14,23] although the opposite result, that WmC20 derivatives are better PI3 kinase inhibitors than Wm have also been described.[22,26] In light of the different reports on the inhibition of PI3 kinase by WmC20 compounds, it is of interest to consider the crystal structure of Wm in the ATP site of PI3 kinase, and what it implies for the self-activating mechanism of action proposed here.

A model of NBD-Wm in the ATP site of PI3 kinase gamma subunit based on earlier crystallographic studies[12] is shown in Figure 4 and provides important support for two key features of the postulate that NBD-WmC20 derivatives are in effect "fluorescent Wm prodrugs." First, when NBD-Wm is formed, it can bind in the ATP site of the kinase similarly to Wm. As shown in Figure 4A, NBD-Wm binds deeply in the ATP pocket, while NBD (cyan) protrudes far out into the solvent, consistent with similar IC50s for PI3 kinase that result when NBD is attached to Wm (Table 1). Second, WmC20 derivatives should not be able to bind in the ATP site of the kinase, a possibility examined in Figure 4B. An NBD-Wm modified at C20 cannot bind to PI3 kinase because of the proximity of the surface of the enzyme shown in blue. Other aspects of the Wm binding to PI3 kinase not shown in Figure 4 indicate a deeply buried C20 is essential for formation of important stabilizing hydrogen bonds between (i) the carbonyl oxygen at the C3 of Wm and hydroxyl group of S806 and (ii) between the hydroxyl group at C6 and an oxygen of D964.[12] As shown in Figure 1, C3 and C6 are positioned close to the reactive C20.

As summarized in Figure 5, the behavior of NBD-Wm C20 derivatives in the PI3 kinase assays (5A) and antiproliferative assay (5B) depends on a combination of assay duration and the rate of release of NBD-Wm. In the 0.5 h kinase assay, the fast activating (**4c**) and slow activating (**4a**, **6a**) NBD-WmC20 derivatives partially generate NBD-Wm **3** and have higher IC50s (are weaker) than the non-C20-protected NBD-Wm. NBD-Wm does not have to self-activate and therefore has a lower IC50. Non-Wm forming compounds (**4b**, **6b**) failed to inhibit PI3 kinase. If NBD-Wm is added to culture media (Figure 5B), reactions occur at the nonprotected C20 position with nucleophiles like amino acids as previously described[28] and as shown in Figure 5B. An uncontrolled mixture of NBD-WmC20 compounds is formed, components of which slowly generate

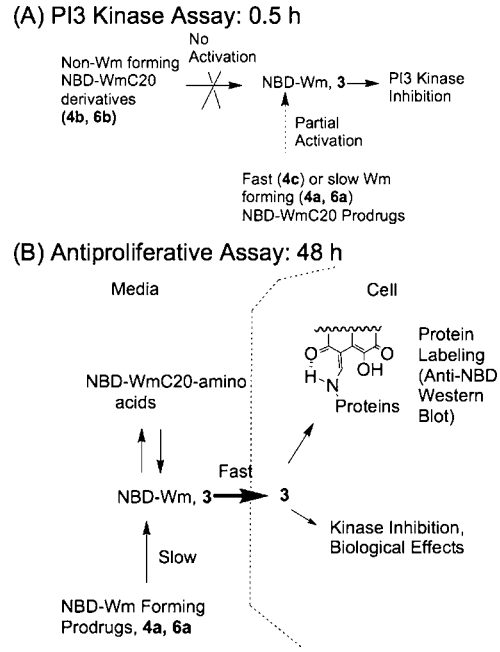

Figure 5. Fate of NBD-WmC20 derivatives in the PI3 kinase and antiproliferative assay. (A) PI3 kinase assay: With a 0.5 h incubation, fast and slow activating WmC20 derivatives partially activate by generating NBD-Wm **3** and have higher IC50s than non-C20-protected forms of Wm like **3**. **3** is stable and active under these conditions and has a low IC50. (B) Antiproliferative assay: NBD-Wm in culture media reacts with nucleophiles like amino acids, yielding a mixture of NBD-WmC20, components of which slowly regenerate NBD-Wm, endowing the culture media with a continuing antiproliferative activity though NBD-Wm has disappeared. When a slowly NBD-Wm forming prodrug (**4a** or **6a**) is used, the viridin NBD-Wm forms over the assay period. The slow formation of **4a** or **6a** an increased potency relative to **3**, although the slow formation of NBD-Wm makes these compounds poor PI3 kinase inhibitors. NBD-Wm rapidly enters cells after release.

Wm, endowing the culture media with a continuing antiproliferative activity though NBD-Wm has disappeared. When a slowly NBD-Wm forming compound (**4a** or **6a**) is added, NBD-Wm slowly forms over the assay period, which is about 5 half-times (48/9). Cell fluorescence increases slowly (Figure 3B) and wortmannylated proteins form slowly (Figure 2), indicating the rate limiting step in culture media with these compounds is the slow release of NBD-Wm. Thus, WmC20 derivatives that behave as slow release, self-activating prodrugs exhibit an improved antiproliferative activity, although they are relatively poor PI3 kinase inhibitors.

Results with the slow Wm forming, dextran conjugate **6a** are of particular interest for two general reasons. First, with **6a** the formation of NBD-Wm **3** is associated with a drastic change in physical properties. When present as the **6a** prodrug, NBD-Wm has a molecular weight of 72 kDa and is hydrophilic and water soluble, properties conferred by its attachment to the 70 kDa dextran carrier. Released from **6a**, NBD-Wm (MW = 677 Da) is poorly soluble in water. Therefore, with **6a**, predominant release of NBD-Wm is extracellular and the released NBD-Wm undergoes a rapid cellular uptake. Supporting this view is the fact that when NBD-Wm is attached to dextran with a nonreleasing linkage (**6b**), it exhibited no antiproliferative activity and failed to enter cells, both by the cell fluorescence and modified protein assays. A second reason for focusing on **6a** is that when used in vivo, the dextran can be an inert macromolecular carrier, extending blood half-time, slowing hepatic uptake, and providing enhanced tumor targeting due to the enhanced permeability and retention effect.[33,34] It should

be noted that the A549 tumor cells used here internalize fluorescent dextrans very poorly (unpublished observations), so that the slow extracellular release of NBD-Wm, followed by uptake of NBD-Wm, is the predominant pathway of NBD-Wm internalization. However, if **6a** is exposed to other types of cells (e.g., monocytes or macrophages after IV injection), **6a** might be internalized intact with an intracellular NBD-Wm release). The results obtained with **6a,** termed the SAV prodrug (self-activating viridin prodrug), in animal models of cancer and inflammation will be presented shortly.

Our slow release mechanism shown in Figure 5A,B provides a basis for two recommendations for selecting Wm or Wm derivatives to analyze signal transduction pathways. For short-duration assays (minutes to about 1 h), Wm should be used because WmC20 derivatives are inactive and will fail to form Wm during these time periods, as evident from results with our PI3 kinase assay. In addition, Wm's lack of charge and hydrophobicity allows it to enter cells rapidly, as was the case for the minimally charged NBD-Wm (Figure 3B). For assays where long incubations are employed, greater than about 6 h, a slowly Wm forming, C20 protected Wm should be used. For animal studies or pharmaceutical applications, WmC20 derivatives are also recommended. As indicated by Wm half-time of less than 10 min in culture media,[35] the use of unprotected, C20 reactive Wm will result in the formation of an uncontrolled mixture of WmC20 compounds, which can give rise to variable results, depending not on the design of the compound but on the nucleophiles present in the media it encounters.

The improved potency as antiproliferative agents of compounds like **6a** is related to their mechanism of slow self-activation and generation of active NBD-Wm **3**, and neither implies nor requires that PI3 kinase be the molecular target of the released NBD-Wm. Our use of the PI3 kinase assay and antiproliferative assay to assess the bioactivity was based on the incubation times employed by these assays, and by their use in many laboratories, rather than a mechanistic relationship between them. In fact determining the molecular target responsible for Wm's inhibition of cell proliferation is complicated by the micromolar concentrations necessary to achieve this effect, see Table 1 and refs 15, 16, 22 These concentrations are considerably above the IC50s of Wm not only for PI3 kinase (IC50 = 1−5 nM)[2,3,8] but also for polo-like kinase (IC50 = 24 nM[4]), mTOR (IC50 = 200 nM[5]), DNA-dependent protein kinase (IC50 = 200 nM)[6] and ATM (IC50 = 200 nM[7]). A second observation for the specificity of Wm for PI3 kinase in vivo was its selective modification of the p110 subunit of PI3 kinase from neutrophils.[13,36] However, more recent studies with a variety of fluorescent Wm derivatives and cancer cell lines have shown Wm can label multiple cell proteins.[4,29,37] Our assay for wortmannylated cell protein (Figure 3A) does not assume that the labeled bands visualized (bands at 35, 55, and 75 kDa) are involved in generating the biological effects of Wm. Instead, this assay assumes that the degree of modification of these proteins provides a quantitative indication of the exposure of the cell to the chemically reactive C20 of NBD-Wm, in much the same way that the level of glucose modified proteins like hemoglobin AIc can be used as an indication of the exposure of cells to glucose.[38]

Wm's unique chemistry, the ability to attach the NBD fluorochrome to the C11 carbon and then further modify Wm at C20, permits the design of fluorescent WmC20 derivatives which self-activate to produce the active NBD-Wm **3** and whose disposition in biological systems can be readily ascertained. The chemistry outlined here can be expanded to obtain more chemically diverse NBD-Wm releasing libraries of compounds whose physical properties or interaction with molecular targets could be determined by replacing the amino-dextran of **6a** with polysaccharides, peptides, antibodies, etc. The ability to rapidly determine the fate of such materials in vivo could then be based on NBD's fluorescence or immunoreactivity, providing a preliminary assessment of a compound's biodistribution and pharmacokinetic properties. Because man-made kinase inhibitors achieve selectivity by binding to the active sites of target kinases with high affinity, the delivery-based design of self-activating Wm natural product prodrugs can be a completely distinct and therefore valuable approach to obtaining kinase inhibitors.

Acknowledgment. Work was supported in part by NIH grants T32P50-CA86355, RO1-EB004472, and T32-CA079443. There are no competing financial interests.

References

(1) Wipf, P.; Halter Robert, J. Chemistry and biology of wortmannin. *Org. Biomol. Chem.* **2005**, *3*, 2053–2061.

(2) Powis, G.; Bonjouklian, R.; Berggren, M. M.; Gallegos, A.; Abraham, R.; Ashendel, C.; Zalkow, L.; Matter, W. F.; Dodge, J.; Grindey, G.; et al. Wortmannin, a potent and selective inhibitor of phosphatidylinositol-3-kinase. *Cancer Res.* **1994**, *54*, 2419–2423.

(3) Creemer, L. C.; Kirst, H. A.; Vlahos, C. J.; Schultz, R. M. Synthesis and in vitro evaluation of new wortmannin esters: potent inhibitors of phosphatidylinositol 3-kinase. *J. Med. Chem.* **1996**, *39*, 5021–5024.

(4) Liu, Y.; Shreder, K. R.; Gai, W.; Corral, S.; Ferris, D. K.; Rosenblum, J. S. Wortmannin, a widely used phosphoinositide 3-kinase inhibitor, also potently inhibits mammalian polo-like kinase. *Chem. Biol.* **2005**, *12*, 99–107.

(5) Brunn, G. J.; Williams, J.; Sabers, C.; Wiederrecht, G.; Lawrence, J. C., Jr.; Abraham, R. T. Direct inhibition of the signaling functions of the mammalian target of rapamycin by the phosphoinositide 3-kinase inhibitors, wortmannin and LY294002. *EMBO J.* **1996**, *15*, 5256–5267.

(6) Hartley, K. O.; Gell, D.; Smith, G. C.; Zhang, H.; Divecha, N.; Connelly, M. A.; Admon, A.; Lees-Miller, S. P.; Anderson, C. W.; Jackson, S. P. DNA-dependent protein kinase catalytic subunit: a relative of phosphatidylinositol 3-kinase and the ataxia telangiectasia gene product. *Cell* **1995**, *82*, 849–856.

(7) Sarkaria, J. N.; Tibbetts, R. S.; Busby, E. C.; Kennedy, A. P.; Hill, D. E.; Abraham, R. T. Inhibition of phosphoinositide 3-kinase related kinases by the radiosensitizing agent wortmannin. *Cancer Res.* **1998**, *58*, 4375–4382.

(8) Knight, Z. A.; Gonzalez, B.; Feldman, M. E.; Zunder, E. R.; Goldenberg, D. D.; Williams, O.; Loewith, R.; Stokoe, D.; Balla, A.; Toth, B.; Balla, T.; Weiss, W. A.; Williams, R. L.; Shokat, K. M. A pharmacological map of the PI3-K family defines a role for p110alpha in insulin signaling. *Cell* **2006**, *125*, 733–747.

(9) Ward, S. G.; Finan, P. Isoform-specific phosphoinositide 3-kinase inhibitors as therapeutic agents. *Curr. Opin. Pharmacol.* **2003**, *3*, 426–34.

(10) Vlahos, C. J.; Stancato, L. F. Inhibitors of cellular signaling targets: designs and limitations. *Methods Mol. Biol.* **2004**, *273*, 87–102.

(11) Ruckle, T.; Schwarz, M. K.; Rommel, C. PI3Kgamma inhibition: towards an "aspirin of the 21st century". *Nat. Rev. Drug Discovery* **2006**, *5*, 903–918.

(12) Walker, E. H.; Pacold, M. E.; Perisic, O.; Stephens, L.; Hawkins, P. T.; Wymann, M. P.; Williams, R. L. Structural determinants of phosphoinositide 3-kinase inhibition by wortmannin, LY294002, quercetin, myricetin, and staurosporine. *Mol. Cell* **2000**, *6*, 909–919.

(13) Wymann, M. P.; Bulgarelli-Leva, G.; Zvelebil, M. J.; Pirola, L.; Vanhaesebroeck, B.; Waterfield, M. D.; Panayotou, G. Wortmannin inactivates phosphoinositide 3-kinase by covalent modification of Lys-802, a residue involved in the phosphate transfer reaction. *Mol. Cell. Biol.* **1996**, *16*, 1722–1733.

(14) Norman, B. H.; Shih, C.; Toth, J. E.; Ray, J. E.; Dodge, J. A.; Johnson, D. W.; Rutherford, P. G.; Schultz, R. M.; Worzalla, J. F.; Vlahos, C. J. Studies on the mechanism of phosphatidylinositol 3-kinase inhibition by wortmannin and related analogs. *J. Med. Chem.* **1996**, *39*, 1106–1111.

(15) Schultz, R. M.; Merriman, R. L.; Andis, S. L.; Bonjouklian, R.; Grindey, G. B.; Rutherford, P. G.; Gallegos, A.; Massey, K.; Powis, G. In vitro and in vivo antitumor activity of the phosphatidylinositol-3-kinase inhibitor, wortmannin. *Anticancer Res.* **1995**, *15*, 1135–1139.

(16) Lemke, L. E.; Paine-Murrieta, G. D.; Taylor, C. W.; Powis, G. Wortmannin inhibits the growth of mammary tumors despite the existence of a novel wortmannin-insensitive phosphatidylinositol-3-kinase. *Cancer Chemother. Pharmacol.* **1999**, *44*, 491–497.
(17) Wiesinger, D.; Gubler, H. U.; Haefliger, W.; Hauser, D. Antiinflammatory activity of the new mould metabolite 11-desacetoxy-wortmannin and of some of its derivatives. *Experientia* **1974**, *30*, 135–136.
(18) Wymann, M. P.; Bjorklof, K.; Calvez, R.; Finan, P.; Thomast, M.; Trifilieff, A.; Barbier, M.; Altruda, F.; Hirsch, E.; Laffargue, M. Phosphoinositide 3-kinase gamma: a key modulator in inflammation and allergy. *Biochem. Soc. Trans.* **2003**, *31*, 275–280.
(19) Laffargue, M.; Calvez, R.; Finan, P.; Trifilieff, A.; Barbier, M.; Altruda, F.; Hirsch, E.; Wymann, M. P. Phosphoinositide 3-kinase gamma is an essential amplifier of mast cell function. *Immunity* **2002**, *16*, 441–451.
(20) Finan, P. M.; Thomas, M. J. PI 3-kinase inhibition: a therapeutic target for respiratory disease. *Biochem. Soc. Trans.* **2004**, *32*, 378–382.
(21) Zhu, T.; Gu, J.; Yu, K.; Lucas, J.; Cai, P.; Tsao, R.; Gong, Y.; Li, F.; Chaudhary, I.; Desai, P.; Ruppen, M.; Fawzi, M.; Gibbons, J.; Ayral-Kaloustian, S.; Skotnicki, J.; Mansour, T.; Zask, A. Pegylated wortmannin and 17-hydroxywortmannin conjugates as phosphoinositide 3-kinase inhibitors active in human tumor xenograft models. *J. Med. Chem.* **2006**, *49*, 1373–1378.
(22) Ihle, N. T.; Williams, R.; Chow, S.; Chew, W.; Berggren, M. I.; Paine-Murrieta, G.; Minion, D. J.; Halter, R. J.; Wipf, P.; Abraham, R.; Kirkpatrick, L.; Powis, G. Molecular pharmacology and antitumor activity of PX-866, a novel inhibitor of phosphoinositide-3-kinase signaling. *Mol. Cancer Ther.* **2004**, *3*, 763–772.
(23) Norman, B. H.; Paschal, J.; Vlahos, C. J. Synthetic studies on the furan ring of wortmannin. *Bioorg. Med. Chem. Lett.* **1995**, *5*, 1183–1186.
(24) Baggiolini, M.; Dewald, B.; Schnyder, J.; Ruch, W.; Cooper, P. H.; Payne, T. G. Inhibition of the phagocytosis-induced respiratory burst by the fungal metabolite wortmannin and some analogues. *Exp. Cell Res.* **1987**, *169*, 408–418.
(25) Yano, H.; Nakanishi, S.; Kimura, K.; Hanai, N.; Saitoh, Y.; Fukui, Y.; Nonomura, Y.; Matsuda, Y. Inhibition of histamine secretion by wortmannin through the blockade of phosphatidylinositol 3-kinase in RBL-2H3 cells. *J. Biol. Chem.* **1993**, *268*, 25846–25856.
(26) Wipf, P.; Minion, D. J.; Halter, R. J.; Berggren, M. I.; Ho, C. B.; Chiang, G. G.; Kirkpatrick, L.; Abraham, R.; Powis, G. Synthesis and biological evaluation of synthetic viridins derived from C(20)-heteroalkylation of the steroidal PI-3-kinase inhibitor wortmannin. *Org. Biomol. Chem.* **2004**, *2*, 1911–1920.
(27) Yuan, H.; Luo, J.; Weissleder, R.; Cantley, L.; Josephson, L. Wortmannin-C20 conjugates generate wortmannin. *J. Med. Chem.* **2006**, *49*, 740–747.
(28) Yuan, H.; Barnes, K. R.; Weissleder, R.; Cantley, L.; Josephson, L. Covalent reactions of wortmannin under physiological conditions. *Chem. Biol.* **2007**, *14*, 321–328.
(29) Barnes, K. R.; Blois, J.; Smith, A.; Yuan, H.; Reynolds, F.; Weissleder, R.; Cantley, L. C.; Josephson, L. Fate of a Bioactive Fluorescent Wortmannin Derivative in Cells. *Bioconjugate Chem.* **2007**, *19*, 130–137.
(30) Gray, A.; Olsson, H.; Batty, I. H.; Priganica, L.; Peter Downes, C. Nonradioactive methods for the assay of phosphoinositide 3-kinases and phosphoinositide phosphatases and selective detection of signaling lipids in cell and tissue extracts. *Anal. Biochem.* **2003**, *313*, 234–245.
(31) Koch, A. M.; Reynolds, F.; Kircher, M. F.; Merkle, H. P.; Weissleder, R.; Josephson, L. Uptake and metabolism of a dual fluorochrome Tat-nanoparticle in HeLa cells. *Bioconjugate Chem.* **2003**, *14*, 1115–1121.
(32) Koch, A. M.; Reynolds, F.; Merkle, H. P.; Weissleder, R.; Josephson, L. Transport of surface-modified nanoparticles through cell monolayers. *ChemBioChem* **2005**, *6*, 337–345.
(33) Vicent, M. J.; Duncan, R. Polymer conjugates: nanosized medicines for treating cancer. *Trends Biotechnol* **2006**, *24*, 39–47.
(34) Duncan, R. Polymer conjugates as anticancer nanomedicines. *Nat. Rev. Cancer* **2006**, *6*, 688–701.
(35) Holleran, J. L.; Egorin, M. J.; Zuhowski, E. G.; Parise, R. A.; Musser, S. M.; Pan, S. S. Use of high-performance liquid chromatography to characterize the rapid decomposition of wortmannin in tissue culture media. *Anal. Biochem.* **2003**, *323*, 19–25.
(36) Thelen, M.; Wymann, M. P.; Langen, H. Wortmannin binds specifically to 1-phosphatidylinositol 3-kinase while inhibiting guanine nucleotide-binding protein-coupled receptor signaling in neutrophil leukocytes. *Proc. Natl. Acad. Sci. U.S.A.* **1994**, *91*, 4960–4964.
(37) Yee, M. C.; Fas, S. C.; Stohlmeyer, M. M.; Wandless, T. J.; Cimprich, K. A. A cell-permeable, activity-based probe for protein and lipid kinases. *J. Biol. Chem.* **2005**, *280*, 29053–29059.
(38) Koenig, R. J.; Peterson, C. M.; Jones, R. L.; Saudek, C.; Lehrman, M.; Cerami, A. Correlation of glucose regulation and hemoglobin AIc in diabetes mellitus. *N. Engl. J. Med.* **1976**, *295*, 417–420.

JM800374F